Campbell et al. Geotherm Energy (2016) 4:9
DOI 10.1186/s40517-016-0051-y

Geothermal Energy

RESEARCH

Open Access

# Geothermal energy from the Main Karoo Basin? New insights from borehole KWV-1 (Eastern Cape, South Africa)

Stuart A. Campbell[1], Philipp Mielke[2] and Annette E. Götz[1*]

*Correspondence: a.e.goetz@keele.ac.uk
[1] School of Physical and Geographical Sciences, Keele University, Staffordshire ST5 5BG, UK
Full list of author information is available at the end of the article

**Abstract**

Deep sedimentary basins are currently being assessed globally with respect to their geothermal energy resources. So far, the utilization of deep geothermal energy has not been addressed or included in any renewable energy scheme of South Africa. However, the Main Karoo Basin, with an area of 700,000 km$^2$ and a basin fill of more than 5000 m of siliciclastic rocks, is a promising target for future enhanced geothermal system (EGS) resource exploration, development and production. Here, we present petro- and thermophysical data from a deep borehole (KWV-1), drilled in 2015 within the framework of the research programme KARIN (Karoo Research Initiative) near the town Willowvale in the Eastern Cape Province. The borehole intersected a 1375 m thick siliciclastic succession of the Permian Ripon Formation up to 2276 m depth. Dolerite sills are characteristic features of the succession, dividing the sedimentary series. The clastic rocks show low matrix permeabilities and high thermal conductivities ranging from 3.17 to 3.71 W/(m·K). Specific heat capacity is highest in siltstones and fine-grained sandstones. Reservoir permeability may be enhanced by joint and fracture systems and dolerite sills with potential for fluid-flow channelling along the intrusion-host rock interfaces. Temperatures of 80 °C at 2200 m depth indicate a moderately elevated geothermal gradient. Sandstones of the Ripon Formation occurring at >3000 m depths in the southern Eastern Cape region are promising EGS reservoirs with temperatures >100 °C suitable for electricity production in a binary geothermal power plant.

**Keywords:** Geothermal potential, Thermophysical rock properties, Permian, Karoo Basin, South Africa

## Background

Within the global scenario of renewable energy exploitation, geothermal energy has undergone an enormous increase in recent years. Besides high-enthalpy volcanic settings (e.g., Chambefort and Bignall 2016), deep sedimentary basins are currently being assessed globally with respect to their geothermal energy resources (e.g., Eggeling et al. 2011; Zafar and Cutright 2014; Horváth et al. 2015; Lenhardt and Götz 2015; Zhu et al. 2015). The utilization of deep geothermal energy has not been addressed or included in any renewable energy scheme of South Africa. However, the Main Karoo Basin, with an area of 700,000 km$^2$ and a basin fill of more than 5000 m of siliciclastic rocks, is a promising target for future geothermal resource exploration, development and production in

South Africa. Recently, Campbell et al. (2016a) provided a first estimation of the geothermal power generation potential of the Karoo Basin based on petro- and thermophysical data from an outcrop study of Permian sandstones in the Eastern Cape Province, and evaluation of groundwater temperature data and heat flow values from literature. A volumetric approach of the sandstones' reservoir potential led to a first estimation of 2240 TWh (8.0 EJ) of power generation potential within the central and southern parts of the basin.

Here, we present the first petro- and thermophysical data from a deep borehole (KWV-1), drilled in 2015 within the framework of the research programme KARIN (Karoo Research Initiative) near the town Willowvale in the Eastern Cape Province (Fig. 1). The aim of the present study is to compare this dataset with the dataset gained from an outcrop analogue to test whether outcrop studies are a reliable tool in geothermal reservoir characterization. Furthermore, the data from borehole KWV-1 will serve as an initial reference dataset for further investigations of the geothermal potential of the Karoo Basin for future exploration of geothermal energy with respect to power generation in South Africa.

## Geological setting

The Karoo Basin of South Africa forms part of a series of basins that developed through subduction, compression, collision, and terrane accretion along the southern margin of Gondwana (Cole 1992; De Wit and Ransome 1992; Veevers et al. 1994; Johnson et al. 1997; Catuneanu et al. 1998). These include the Paraná Basin in South America, the Beacon Basin in Antarctica and the Bowen Basin in Australia, depocentres filled between

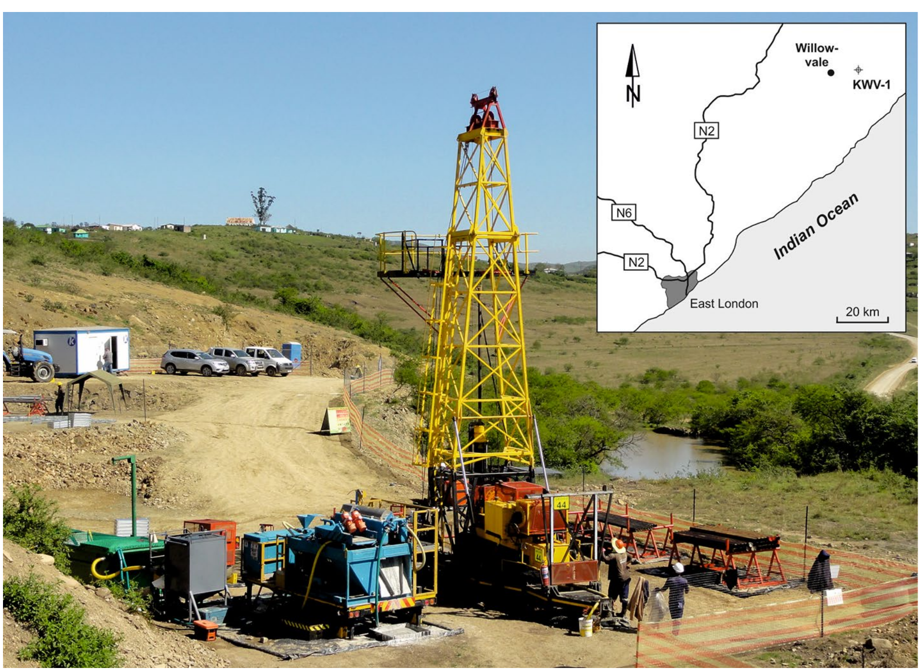


**Fig. 1** Drill site of borehole KWV-1, drilled in 2015 within the framework of the research programme KARIN (Karoo Research Initiative) near the town Willowvale in the Eastern Cape Province, South Africa (32°14′43.10″ S, 28°35′08.10″ E; 263 m a.s.l.). The final depth of borehole KWV-1 is 2352.39 mbs

the Late Carboniferous (Pennsylvanian) and Mid Jurassic. Their economic significance in terms of energy resources ranges from coal and coal bed methane to shale gas, uranium and geothermal energy (Hancox and Götz 2014).

Recent interpretations of the basin evolution and its tectonic setting range from a retro-arc foreland basin (Catuneanu et al. 1998, 2002; Catuneanu 2004; Veevers 2004; Johnson et al. 2006), a transtensional foreland system created by subsidence and tilting in a strike-slip regime (Tankard et al. 2009), a thin-skinned fold belt that developed from collisional tectonics and distant subduction to the south (Lindeque et al. 2011), to a transient hypothetical mantle plume related model (Turner 1999).

The Karoo Basin is underlain by a stable basement comprising the Kaapvaal Craton in the north (Nguuri et al. 2001; James et al. 2003), the Namaqua-Natal Metamorphic Belt in the south (Cornell et al. 2006) and the Cape Fold Belt along its southern margin (Fig. 2; Johnson et al. 2006). The Namaqua-Natal Metamorphic Belt (NNMB) is defined as those terranes in Southern Africa which acquired a pervasive structural fabric during the ca. 1.1 Ga Kibaran tectono-magmatic event (Thomas et al. 1993). The Natal Belt makes up the eastern section of the Namaqua-Natal Metamorphic Belt and lies adjacent to the south-eastern margin of the Kaapvaal Craton. It is divided, from north to south, into the Tugela, Mzumbe and Margate terranes. The Margate terrane is the structurally highest panel and is characterized by granulite facies rocks. The underlying Mzumbe terrane comprises gneisses at upper amphibolite and locally granulite facies and the Tugela terrane rocks at amphibolite and greenschist facies (McCourt et al. 2006). Heat flow values recorded from the Kaapvaal Craton are ultra-low (33 $mW/m^2$) and low to moderately high (50–75 $mW/m^2$) in the surrounding mobile belts (Jones 1987, 1992, 1993, 2001).

In the Early Palaeozoic (Cambrian-Silurian), sediments of the Cape Supergroup were deposited along a passive continental margin during a period of extensional tectonism. Sedimentation continued into the Late Palaeozoic (Devonian-Carboniferous) and was followed by deposition of the Permo-Triassic Karoo sediments (Hälbich 1983, 1992; Shone and Booth 2005). Tectonic inversion took place towards the end of the Palaeozoic. The Cape Fold Belt developed in response to subduction-related compression along the convergent south-western margin of Gondwana (Trouw and de Wit 1999) resulting in intense deformation of the Cape Supergroup, the underlying basement, as well as lower units of the Karoo Supergroup (Lindeque et al. 2011) by northwards-directed shortening (de Wit and Ransome 1992).

Karoo-aged depositional environments broadly range from glacial (Dwyka Group), to marine and coastal plain (Ecca Group), to non-marine fluvial and aeolian (Beaufort and Stormberg groups). These siliciclastic deposits reach a thickness of more than 5 km in the southern part of the basin and are capped by some 1.4 km of basaltic lavas of the Drakensberg Group (Veevers et al. 1994; Johnson et al. 1996), the extrusion of which is related to the break-up of Gondwana (Cox 1992). Flexural tectonics imposed by orogenic loading and dynamic subsidence are the most important controls on accommodation in the Karoo Basin (Catuneanu 2004). Initial flexural tectonics resulted in partitioning of the foreland system into foredeep, forebulge and back-bulge flexural provinces. Later in the evolution of the Karoo Basin, flexural tectonics was supplemented by dynamic subsidence, which created additional accommodation across the entire foreland system.

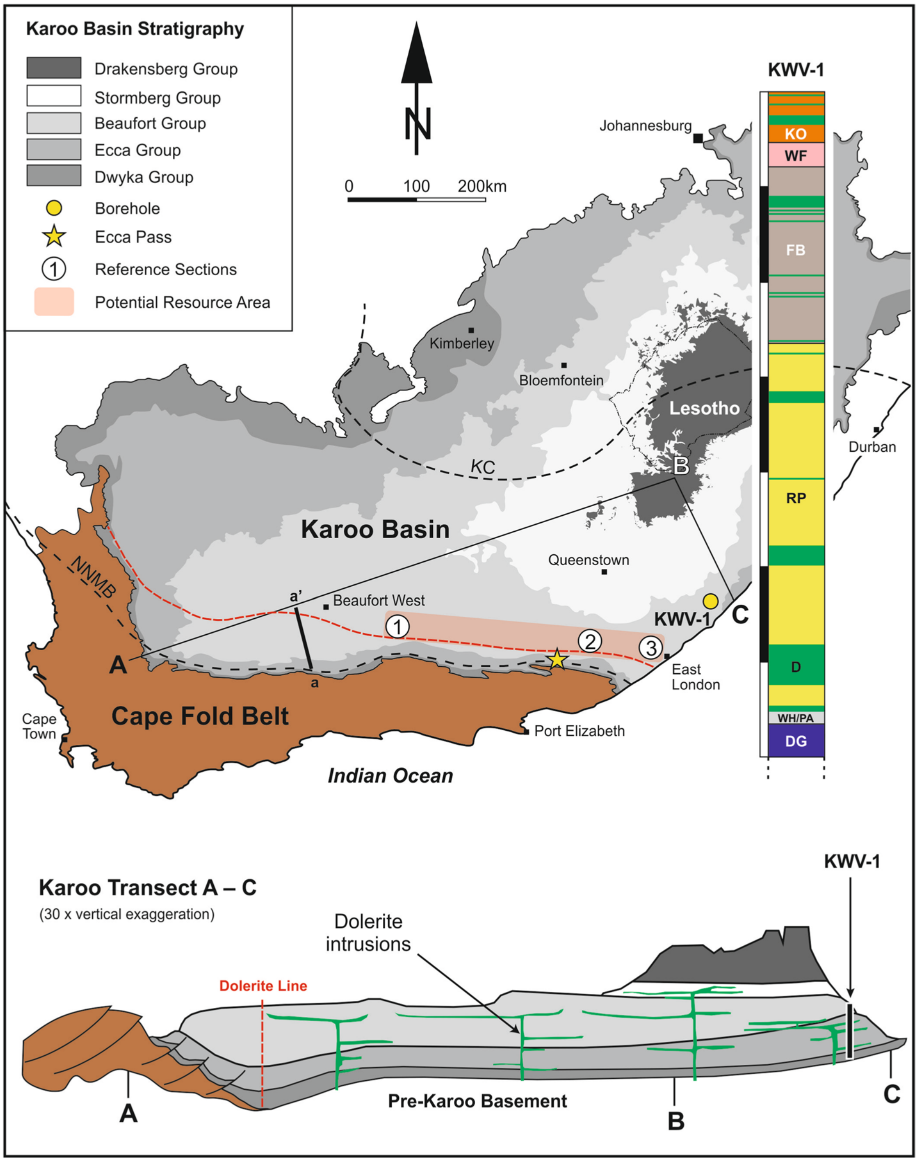


**Fig. 2** Geological map of the Karoo Basin with location of borehole KWV-1 (east of the town Willowvale, Eastern Cape Province; see Fig. 1), stratigraphic reference sections 1–3 (see Fig. 3) intersecting the Ripon Formation at depths >3000 m, seismic reflection profile *a–a'* (Fig. 6), and stratigraphic log of KWV-1 (*KO* Koonap Formation, *WF* Waterford Formation, *FB* Fort Brown Formation, *RP* Ripon Formation, *D* Dolerite, *WH* Whitehill Formation, *PA* Prince Albert Formation, *DG* Dwyka Group), *scale bars* 350 m. *Transparent rectangle* west of East London marks the potential resource area. Transect **A**–**C** highlights the layer cake stratigraphy of the Karoo Basin with dolerite sills and dykes and location of borehole KWV-1 intersecting the uppermost Dwyka, entire Ecca, and lowermost Beaufort groups. *Red dashed line* marks the southern extent of dolerite intrusions (*dolerite line*; Veevers et al. 1994). *Black dashed lines* mark the craton boundaries of the Kaapvaal Craton (*KC*) in the north (Nguuri et al. 2001; James et al. 2003) and the Namaqua-Natal Metamorphic Belt (NNMB) in the south (Cornell et al. 2006) adjacent to the Cape Fold Belt, forming the basement of the Karoo Basin

The configuration of the earliest Karoo foreland system accounts for a forebulge elevated above the base level during Dwyka times, representing the early underfilled stage followed by a time of system-wide sedimentation during Ecca times (late underfilled stage), when the forebulge subsided below the base level under the influence of dynamic subsidence. During the entire underfilled stage, the foredeep hosted a relatively deep marine environment with glacio-marine (Dwyka) followed by pelagic and gravity flow (lower-middle Ecca) sediments. The upper part of the Ecca Group reflects a filled stage of shallow marine sedimentation followed by the overfilled style of fluvial sedimentation of the overlying Beaufort and Stormberg groups (Catuneanu et al. 2005). The complex basin architecture led to distinct lateral facies changes and varying thicknesses of sedimentary formations (Smith 1990; Smith et al. 1993).

Dolerite sills and dykes occur throughout the Karoo Basin with a southern extent of intrusions marked by the so-called dolerite line (Veevers et al. 1994; Fig. 2). The thickest sills are up to 200 m thick, representing extensive (>200 km) sheets emplaced in the organic-rich shales of the lower Ecca Group. Higher in the Karoo stratigraphy, sills are emplaced in the sandstone-dominated upper Ecca and Beaufort groups and form nested saucer-shaped intrusions with individual thicknesses of about 100 m and characteristic diameters of 20–60 km. At an outcrop-scale and from boreholes a high frequency of intrusions (at intervals of 10 s of meters) is known in these stratigraphic groups (Smith 1990). Sills are less common in the uppermost part of the basin, the Stormberg Group (Smith 1990; Johnson et al. 1996; Catuneanu et al. 2005), whereas dykes are common and form 120–180 km long lineaments such as the 100–200 m wide Gap Dykes. Sills are absent in the Drakensberg Group lavas, suggesting that they were emplaced prior to the main phase of flood volcanism or that emplacement within the lavas was prevented. The Karoo sills are dominantly tholeiitic basalts to basaltic andesites, although more evolved sills are also present locally (Marsh and Eales 1984; Neumann et al. 2011). Recently published U–Pb zircon data (Svensen et al. 2012) indicate that basin-scale emplacement took place within an interval of less than 0.5 Ma and could represent a single magma emplacement event. The peak of volcanic activity in South Africa and Lesotho is recorded at 183 ± 1 Ma by 40Ar/39Ar dating of the Drakensberg basalts and some Karoo Basin dykes and sills (Duncan et al. 1997; Jourdan et al. 2005, 2007).

The Ripon Formation is part of the Permian Ecca Group and recently published U–Pb zircon ages from the Ecca Pass section (McKay et al. 2015) place the formation chronostratigraphically in the Mid Permian (early Guadalupian). It is generally 600–700 m thick but increases in thickness to over 1000 m in the eastern part of its outcrop area and rapidly wedges out northwards in the subsurface (Veevers et al. 1994; Johnson et al. 2006). A thickness of >1350 m was encountered in the study area northeast of East London (Fig. 2). The formation is composed of poorly-sorted medium to fine-grained sandstones, alternating with siltstones and shales, and occurs at depths between 1000 and >3500 m in the southern part of the Karoo Basin (Fig. 3). Ecca shales below the Ripon Formation in the south-western part of the basin proximal to the Cape Fold Belt document a thermal history with temperatures >230 °C (Craddock et al. 2007). Vitrinite reflectance values of these shales of >3.5 % were reported by Branch et al. (2007) and Campbell et al. (2016b) from the south-western basin, and from the south-central to south-eastern part of the basin Decker (2011) reports values of <3.5 % (≤200 °C). In the East London area (south-eastern basin) depths of the Ripon Formation in excess of 4500 m can be expected due to down-faulting (Scheiber-Enslin et al. 2015). An area of 16,000 km$^2$, marked as a transparent rectangle west of East London (Fig. 2), where

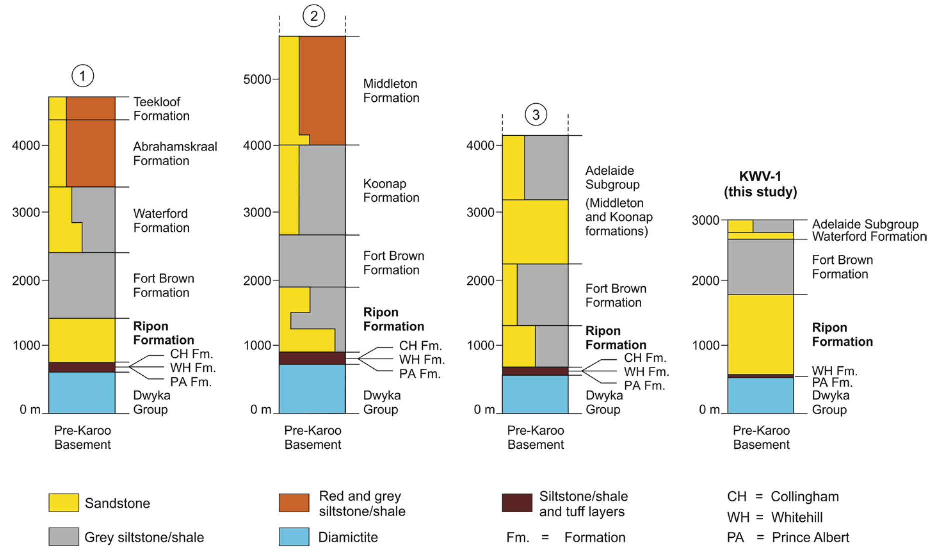


**Fig. 3** Stratigraphic reference sections (1–3) of the Permian Ecca Group (Prince Albert, Whitehill, Collingham, Ripon, Fort Brown and Waterford formations) and lower Beaufort Group (Middleton, Koonap, Abrahamskraal and Teekloof formations) in the Eastern Cape (for location of sections see Fig. 2), compiled and modified from Johnson et al. (2006) and Steyl et al. (2012), and stratigraphic section intersected in borehole KWV-1 (this study). The Ripon Formation contains the first sandstones within the Ecca Group, after deposition of glaciomarine tillites (Dwyka Group) and shallow to deep marine shales of the Prince Albert, Whitehill and Collingham formations (lowermost Ecca Group) on the Pre-Karoo Basement. The formation is composed of poorly-sorted medium to fine-grained sandstones, alternating with siltstones and shales, and occurring at depths between 1000 and >3500 m in the southern part of the Karoo Basin

boreholes documented Ripon sandstones at depths >3000 m (Fig. 3), is identified as a potential resource area and in this study relevant to a first estimation of the theoretically available thermal energy (heat in place).

The average thickness of sandstone units in the formation is ca. 12 m with an average minimum and maximum of 0.3 and 44 m, respectively. The Ripon sandstones of the Eastern Cape region are interpreted as turbidites (Johnson et al. 2006; Campbell 2014) and represent the stratigraphic equivalent of the Skoorsteenberg and Laingsburg formations in the Western Cape region (Johnson et al. 1996, 1997; Catuneanu et al. 2002) which have been studied in detail as outcrop analogues of hydrocarbon reservoirs (e.g., Flint et al. 2011; Brunt et al. 2013). In the study area northeast of East London (Fig. 2) the Ripon Formation is dominated by sandstones and might represent the southernmost deposits of the Natal Trough (Tankard et al. 1982; Selley 1997). The sandstone succession is highly fractured and intersected by numerous dolerite sills reaching a maximum thickness of 148 m. Vertical and sub-vertical fractures, associated with dolerite sills and dykes, occurring at depths >3000 m are documented in SOEKOR exploration boreholes (e.g., Leith and Trümpelmann 1967). In outcrops, two predominant mean joint orientations of 242/53 and 143/73 were encountered (Campbell 2014) and similar orientations are reported from the overlaying Permo-Triassic Beaufort sandstones studied by Senger et al. (2015). Major faults in the study area northeast of East London are striking E–W (Mountain 1974; Johnson and Caston 1979).

## Methods

The studied borehole KWV-1 was drilled in an abandoned quarry 10 km E of the town Willowvale (Fig. 1) in the Eastern Cape Province, South Africa (32°14′43.10″ S, 28°35′08.10″ E; 263 m a.s.l.) within the framework of the research programme KARIN (Karoo Research Initiative) and represents the first deep Karoo borehole since the SOEKOR exploration drilling program undertaken in the 1960s and 1970s. The core is curated at the Council for Geoscience (CGS), Pretoria. The borehole intersected six formations of the Beaufort and Ecca groups and the Dwyka Group (Fig. 2): the Koonap Formation of the Adelaide Subgroup (lower Beaufort Group) at 0 m, the Waterford Formation at 189.20 m below surface (mbs), the Fort Brown Formation at 264.50 mbs, the Ripon Formation including the Trumpeters Member at 919.20 mbs, the Wonderfontein Member at 1048.40 mbs, and the Pluto's Vale Member at 1346.13 mbs, the Whitehill Formation at 2294.95 mbs, the Prince Albert Formation at 2308.40 mbs (Ecca Group), and the Dwyka Group at 2339.75 mbs. The final depth of borehole is 2352.39 mbs. Core size PQ (85 mm) was used until a depth of 300.16 m, core size HQ (63.5 mm) until a depth of 1000.15 m, and core size NQ (47.6 mm) until the end of hole.

In total, 32 samples were selected across all members (Trumpeters Member, Wonderfontein Member, and Pluto's Vale Member) of the Ripon Formation (Fig. 4). Lithologies range from siltstone to very fine to medium-grained, partly organic-rich sandstone (Fig. 5). Descriptions of the samples were prepared, detailing lithology as well as the occurrence of pore space and fractures. Petrographic analyses were conducted on thin sections prepared from selected samples at Keele University. Measurements of petro- and thermophysical rock properties were performed at the Geothermal Laboratory *Hydrothermikum* at TU Darmstadt.

Porosity and permeability analyses were carried out on all samples. Measurements of skeletal density (helium pycnometer AccuPyc 1330) and envelope density (DryFlo pycnometer GeoPyc 1360) allowed the calculation of total porosity. Permeability measurements were conducted by usage of conditioned compressed air, using a gas pressure columnar-permeameter, developed at the Institute of Applied Geosciences, TU Darmstadt, Germany (Filomena et al. 2014). The device can measure permeability ranges from 1 d to 1 µd ($9.869 \cdot 10^{-13}$–$9.869 \cdot 10^{-19}$ $m^2$). Samples were measured in a 1 MPa confined cell with five pressure stages ranging from 0.108 to 5 MPa, and a differential pressure of 80 kPa. All samples were dried overnight in a conventional oven at 105 °C before the measurements.

For the determination of the dry bulk thermal conductivity $\lambda$ and dry bulk thermal diffusivity $\alpha$, the optical scanning method after Popov et al. (1999) was applied using a Thermal Conductivity Scanner developed by "Lippmann and Rauen GbR". The determination of both properties is based on a comparison of the cooling rates of a pre-heated sample with unknown thermal properties with the cooling rates of reference standards with known thermal properties. The methodology is non-destructive and contactless, but requires the sample surface to be sprayed with a thin layer of black acrylic lacquer to homogenize heating and temperature measurements. The measurement accuracy is stated by the manufacturer as ca. 3 % (c.f. Lenhardt and Götz 2015). Measurements of thermal properties on dry porous samples under laboratory conditions reveal generally lower values than measurements on water-saturated samples of the reservoir. However,

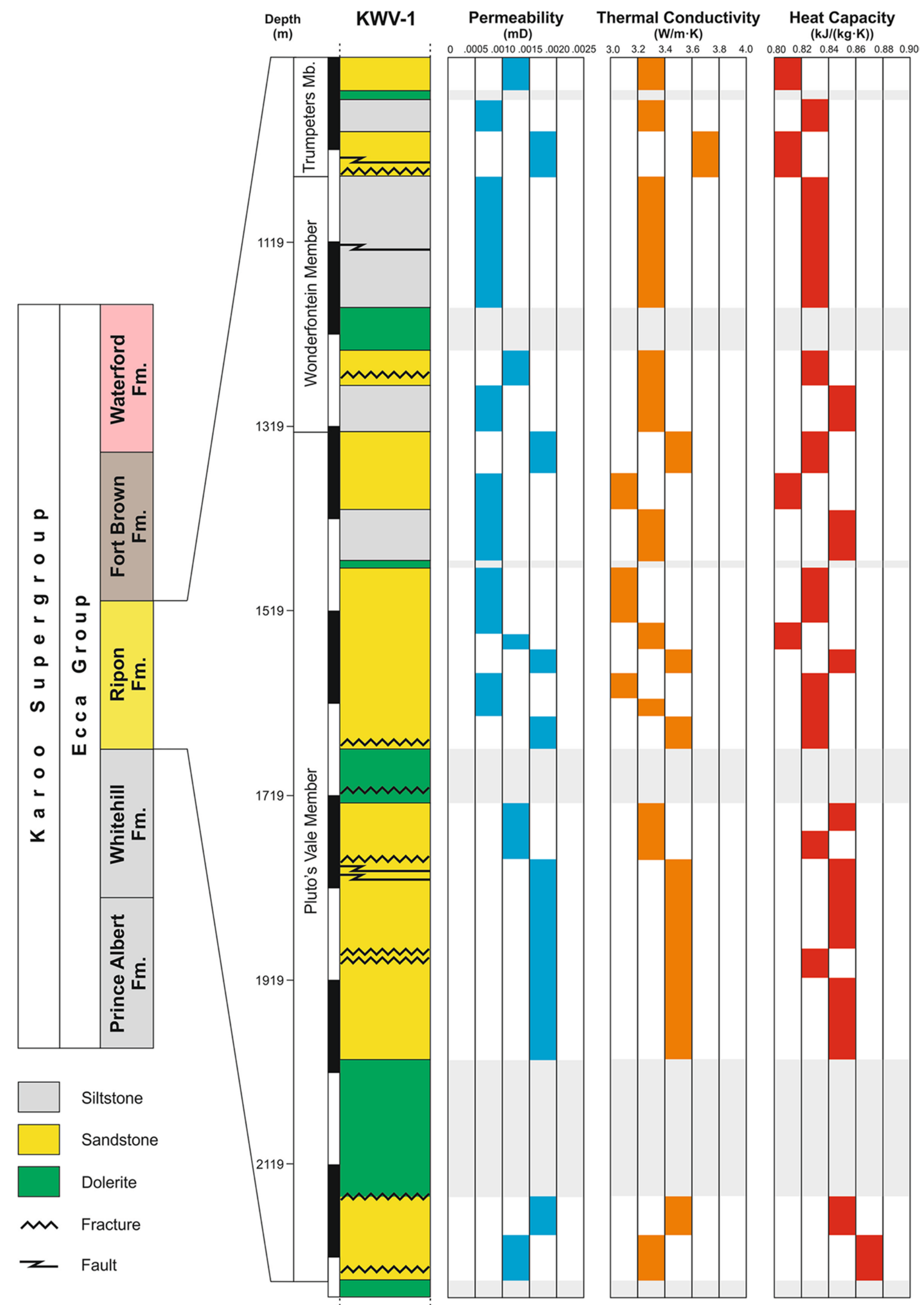


**Fig. 4** Stratigraphic log of the Ripon Formation intersected in borehole KWV-1 and trends of thermophysical properties on a reservoir scale. Intervals without measurements (dolerites) are *grey shaded*. *Scale bars* 100 m, *Fm* Formation. All lithologies are classified as impermeable. Fine-grained sandstones, the dominant lithology, show the highest thermal conductivity. Specific heat capacity reveals the highest values in siltstones and fine-grained sandstones

measurements on oven-dried core samples guarantee a very good reproducibility of the results in contrast to in situ values (Homuth et al. 2014). Including lithotype-specific correction and conversion equations (Fuchs et al. 2013) enable the calculation of

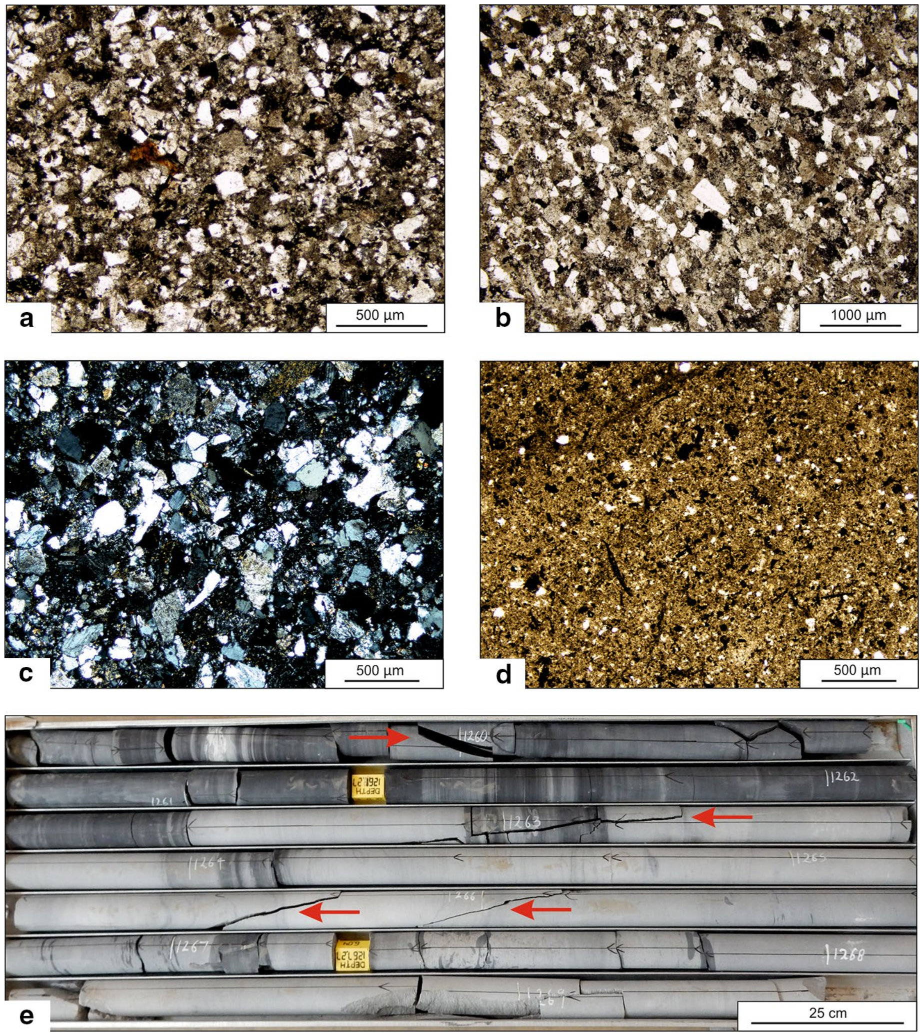


**Fig. 5** Ripon Formation intersected in borehole KWV-1 (32°14′43.10″ S, 28°35′08.10″ E), Eastern Cape Province, South Africa; **a** Very fine to fine-grained feldspathic greywacke containing quartz, feldspar, lithic fragments in clay-sized matrix with organic matter. Plane polarized light; **b** fine-grained lithic arkose containing predominantly quartz, lithic fragments in clay-sized matrix. Plane polarized light; **c** medium-grained lithic arkose consisting of quartz, feldspar, lithic fragments in clay-sized matrix. Cross polarized light; **d** siltstone containing abundant quartz and organic matter. Plane polarized light; **e** sandstones of the Wonderfontein Member between the depths of 1259.50–1269.50 m with sub-vertical fractures (marked by *red arrows*)

the water-saturated matrix (bulk) thermal conductivity from data of dry-measured bulk thermal conductivity, and can be applied in a later stage of exploration to gain more accurate estimates of the resource potential. In contrast, samples of impermeable to low permeability rocks show different effects. In the reservoir, the thermal properties are affected by temperature and pressure. Compaction closes micro-fractures and thus decreases porosity which leads to an increase of bulk density. As a result, thermal conductivity increases due to better grain-to-grain contacts and less "defects" (such as micro-fractures). Increase in temperature causes "thermal cracking" due to differential thermal expansion coefficients of the minerals (Clauser and Huenges 1995). Hence at depth micro-fractures can be assumed, that are not present at ambient (laboratory) conditions. As a result, thermal conductivity decreases due to increasing "defects". Saturation generally enhances thermal conductivity and specific heat capacity in a porous rock, as water/brine has significantly higher values than air. But in a low porous rock there might be simply no pore space that can be filled with water, so the properties are not increased. Petro- and thermophysical rock properties are presented in Table 1.

A dynamic Calvet calorimeter SETARAM C80 (Calvet and Prat 1963) was used to measure the specific heat capacity for the temperature range from 25 to 200 °C. The device has two chambers, of which one is filled with weighted sample material, while the second chamber remains empty and acts as reference. In course of the measurements the temperature was stepwise increased by 0.5 °C/min, while the heat flux in the sample chamber and reference chamber is measured. The difference between the heat flows is proportional to the specific heat capacity of the sample material (Schellschmidt 1999). The device has a temperature accuracy of ±0.1 °C and a measurement precision of ±0.1 %. The specific heat capacity results are presented in Table 2.

## Results

### Lithology and petrography

The Permian Ripon Formation contains siltstone and three distinct sandstone lithologies: (1) very fine-grained sandstones, (2) fine-grained sandstones, and (3) medium-grained sandstones.

Very fine-grained sandstones (Fig. 5a) contain sub-rounded to rounded grains of quartz and feldspar as well as shale fragments in a clay-sized matrix classifying them as feldspathic greywackes (Folk 1954). Feldspars include albite as well as microcline and have been partially altered to clays. Muscovite, biotite and chlorite were also observed within the poorly sorted sandstones.

Fine-grained sandstones (Fig. 5b) contain angular to sub-rounded quartz, albite, microcline, and lithic fragments within a clay-sized matrix classifying them as lithic arkoses (Folk 1954). Chert fragments, zircon, chlorite, and muscovite were also observed within the moderately sorted sandstone. The majority of the feldspar grains had been altered to clays, possibly sericite.

The medium-grained sandstones (Fig. 5c) contain angular to sub-angular quartz, albite, microcline, and lithic fragments within a clay-sized matrix which classify them as lithic arkoses (Folk 1954). Muscovite, chlorite, chert, and hornblende were also observed in the poorly to moderately sorted sandstones. The primary clay content is lower than in the very-fine and fine-grained sandstones, however, the majority of feldspars have been partially altered to clays.

Siltstones (Fig. 5d) contain angular to sub-angular quartz grains, elongate muscovite as well as chert and shale fragments in a clay-sized matrix. Abundant organic particles were also observed.

### Faults and fractures

An 8 cm wide fault was observed at 1046.40 m in the Trumpeters Member sandstone and a 2.5 cm wide fault at 45° to the core axis was encountered at 1121.95 m within the Wonderfontein Member siltstones (Fig. 4). Fault breccias were encountered in sandstones of the Pluto's Vale Member between 1792.60 and 1797.90 m. Pyrite and quartz

**Table 1 Petro- and thermophysical rock properties of the Ripon Formation (southern Karoo Basin, South Africa)**

| Sample location | Number of measurements | Density ($kg/m^3$) | Porosity (%) | Permeability | | Thermal conductivity [W/(m K)] | Thermal diffusivity (1.0 E−06 $m^2/s$) |
|---|---|---|---|---|---|---|---|
| | | | | (mD) | ($m^2$) | | |
| Ecca pass (outcrop) | 76 | 2630–2730 (mean 2670) | 0–3.70 (mean 1.0) | 0.0100–0.1000 (mean 0.0500) | $7.21 \cdot 10^{-18}$–$9.94 \cdot 10^{-17}$ (mean $4.83 \cdot 10^{-17}$) | 2.38–3.20 (mean 2.82) | 0.71–1.83 (mean 1.21) |
| KWV-1 (borehole) | 32 | 2570–2770 (mean 2700) | 0.40–2.20 (mean 1.3) | 0.0010–0.0020 (mean 0.0014) | $9.87 \cdot 10^{-19}$–$1.97 \cdot 10^{-18}$ (mean $1.38 \cdot 10^{-18}$) | 3.17–3.71 (mean 3.37) | 1.30–1.53 (mean 1.39) |

**Table 2 Specific heat capacity values [kJ/(kg·K)] at different temperatures (25, 80, 100, 200 °C) and for extrapolated temperatures at reservoir depths 3000 m (103 °C) and 3500 m (117 °C), respectively**

| Sample location | Lithology | $T = 25$ °C | $T = 80$ °C | $T = 100$ °C | $T = 200$ °C | $T = 103$ °C | $T = 117$ °C |
|---|---|---|---|---|---|---|---|
| KWV-1 (borehole) | Siltstone | 0.80 | 0.88 | 0.91 | 1.06 | 0.92 | 0.94 |
| KWV-1 (borehole) | Very fine-grained sandstone | 0.80 | 0.87 | 0.89 | 1.02 | 0.90 | 0.92 |
| KWV-1 (borehole) | Fine-grained sandstone | 0.80 | 0.86 | 0.88 | 1.00 | 0.88 | 0.90 |
| KWV-1 (borehole) | Medium-grained sandstone | 0.77 | 0.83 | 0.86 | 0.97 | 0.86 | 0.88 |

was observed along fault surfaces. Numerous vertical to sub-vertical fractures (Fig. 5e) occur within the sandstones of the Pluto's Vale, Wonderfontein and Trumpeters members. Fractures in dolerite sills occur at 1715.81 m and between sills and sandstone at 2158 m. Some fractures in both sandstone and dolerite have been filled with gypsum and calcite.

## Petro- and thermophysical rock properties

Ranges and mean values of density, porosity, permeability, thermal conductivity, and thermal diffusivity of the Ripon Formation's silt- and sandstones from borehole KWV-1 are provided in Table 1 in comparison to data gained from outcrop samples from the Ecca Pass section (Campbell et al. 2016a). Specific heat capacity at different temperatures (25, 80, 100, 200 °C) and for extrapolated temperatures at reservoir depths are provided in Table 2.

Siltstones have porosities below 1 %, their permeabilities are below 0.0010 mD ($9.87 \cdot 10^{-19}$ m$^2$), the mean density is 2740 kg/m$^3$. Very fine-grained sandstones range in porosity from 1.2 to 1.3 % with a mean of 1.22 %. Their permeabilities show a mean value of 0.0011 mD ($1.09 \cdot 10^{-18}$ m$^2$), the mean density is 2680 kg/m$^3$. The fine-grained sandstones range in porosity from 0.8 to 1.8 % with a mean of 1.1 %. The permeabilities of this lithology have a mean value of 0.0020 mD ($1.97 \cdot 10^{-18}$ m$^2$), the mean density is 2700 kg/m$^3$. The medium-grained sandstones range in porosity from 1.5 to 2.2 % with a mean of 1.7 %. Their permeabilities are below 0.0010 mD ($9.87 \cdot 10^{-19}$ m$^2$), the mean density is 2650 kg/m$^3$.

The thermal conductivity of the siltstones shows a mean of 3.21 W/(m·K) with a standard deviation of 0.03 W/(m·K), very fine-grained sandstones have a mean of 3.26 W/(m·K) with a standard deviation of 0.04 W/(m·K), fine-grained sandstones exhibit a mean of 3.67 W/(m·K) with a standard deviation of 0.05 W/(m·K), and the thermal conductivity of the medium-grained sandstones shows a mean of 3.19 W/(m·K) with a standard deviation of 0.04 W/(m·K). Heat capacity is highest in siltstones and fine-grained sandstones (Table 2).

## Heat in place

Following the volumetric approach by Muffler and Cataldi (1978), the calculation of the heat in place using Eq. (1) leads to a first estimation of the theoretically available thermal energy from a geothermal system.

$$E_{th} = c_r \cdot \rho_r \cdot V \cdot (T_r - T_s) \quad (1)$$

where $E_{th}$ is heat in place (J), $c_r$ the specific heat capacity of the reservoir rock [kJ/(kg·K)], $\rho_r$ the density of the reservoir rock (kg/m$^3$), $V$ the reservoir volume (m$^3$), $T_r$ the reservoir temperature (°C) and $T_s$ the average surface temperature (°C), respectively.

With the available KWV-1 data of a mean specific heat capacity $c_r$ of 0.89 [kJ/(kg·K)] (Table 2), a mean density $\rho_r$ of 2700 kg/m$^3$ (Table 1), a reservoir volume of 10,400,000,000,000 m$^3$ including the area west of East London to the western border of the Eastern Cape Province north of the Cape Fold Belt (Fig. 2) where the Ripon Formation reaches a mean thickness of 650 m and occurs at depths of 3000 m, and a temperature difference of 85 °C (reservoir temperature $T_r = 103$ °C; average surface temperature $T_s = 18$ °C), a preliminary estimation of the available thermal energy suggests 596.70 TWh (2.15 EJ) of heat in place.

## Discussion

The petro- and thermophysical rock properties of the Ripon Formation intersected in borehole KWV-1 at a depth between 919.20 and 2294.95 m reveal the potential of this formation for geothermal energy utilization. Generally, impermeable fine-grained sandstones—the dominant lithology—show the highest thermal conductivity (3.71 W/(m·K)). Fine-grained sandstones and siltstones revealed the highest specific heat capacity. A comparison of outcrop and core samples shows that measurements of outcrop samples yield slightly higher porosities and permeabilities, however, these sandstones have permeabilities that are low to impermeable (Campbell et al. 2016a). Thermal conductivities of sandstones encountered from borehole KWV-1 are noticeably higher than those of outcrop sandstones. For a first assessment of a potential geothermal resource and its distinct reservoir formations, data gained from outcrop analogue studies seem to lead to a conservative estimation of the reservoir capacity but prove to be useful with respect to transferability of outcrop conditions to reservoir conditions. Based on the investigations of geothermal parameters from a deep drill core, in a later stage of geothermal exploration, the integration of reservoir transfer models (e.g., Tikhomirov 1968; Somerton 1992; Vosteen and Schellschmidt 2003; Abdulagatova et al. 2009) enables a more precise reservoir prognosis including numerical simulation and upscaling (Rühaak et al. 2015).

Another tool for the prognosis of geothermal reservoir properties of deep sedimentary basins is the thermofacies concept introduced by Sass and Götz (2012) who showed that permeability and thermal conductivity, significantly responsible for the heat flow of a reservoir formation, are dependent on the distinct lithofacies type. Applying the thermofacies concept, the Ripon Formation's silt- and sandstones are classified as petrothermal system with conductive heat transfer. Such systems need reservoir stimulation for techno-economic utilization (Tester et al. 2005; Huenges 2010). The high fracture and dolerite sill occurrence in the silt- and sandstones of the Ripon Formation (Figs. 4, 5e) provide a natural permeability improvement that can be enhanced by hydraulic fracturing. The influence of dykes and sills to permeability enhancement was studied by Senger et al. (2015) in the Karoo Basin and demonstrates the potential for fluid-flow channelling along the intrusion-host rock interfaces. This study also highlights the different fracture types based on the likely mode of formation, namely (1) syn-emplacement fractures in host rocks, (2) post-emplacement fractures in dolerite, and (3) tectonic fractures in both host rock and dolerite. These three fracture types are also present in borehole KWV-1. Outcrop data from the Ecca Pass (Campbell 2014) reveal two predominant mean joint orientations of 242/53 and 143/73 in the Permian Ripon Formation and similar orientations were measured in the Permo-Triassic Beaufort sandstones studied by Senger et al. (2015). However, these authors note that open fractures decrease with increasing lithostatic pressure (depth) and are less likely good fluid conduits at depth. Temperatures of 80 °C at 2200 m depth indicate a geothermal gradient of 28.2 °C/km in the Willowvale area (mean annual surface temperature 18 °C) northeast of East London. Sandstones of the Ripon Formation occurring at >3000 m depths in the southern Eastern Cape region (Fig. 3) are thus promising reservoirs with expected temperatures of >100 °C, suitable for electricity production in a binary geothermal power plant. On a local scale, direct use of the potential reservoir is most probably an alternative to harness geothermal energy from the Karoo Basin. Thermal springs reported (Steyl et al. 2012) show water temperatures ranging from 26 to 41 °C, with temperatures of 26 to 31 °C in the southern part, 30 to 37 °C in the central part and 28 to 41 °C in the north-eastern part of the basin. So far, thermal springs have been developed for direct use north of the Karoo Basin in the Limpopo Province north of Pretoria, where water temperatures of up to 71 °C have been reported (Chevallier et al. 2014). A review of the direct utilization of geothermal energy in South Africa is given in Lund and Boyd (2015).

The quantification of the heat in place provided first information for the potential resource area in the Eastern Cape. In a next step, the recoverable thermal energy, considering recovery factors suitable for low porosity rocks, and additionally the potential recoverable electrical energy can be reported for an identified resource as outlined in Limberger et al. (2014).

Heat flow data from the Karoo Basin (Jones 1993, 2001) indicate areas of a moderately elevated heat flow within the basin related to the underlying basement (Namaqua-Natal Mobile Belt; Figs. 2, 6). Generally, heat flow in the mobile belt is much higher than in the Kaapvaal Craton. Preliminary models attribute approximately half the excess heat flow in the Namaqua-Natal Mobile Belt to crustal radioactivity, and the rest to a higher heat flux across the Moho (Jones 1993). Geotherms based on these models agree with estimates of upper mantle pressure–temperature conditions inferred from kimberlite inclusion studies, and indicate that the lithosphere below the Kaapvaal Craton is considerably cooler and thicker than the lithosphere below the Namaqua-Natal Mobile Belt.

Additionally, distinct spatial patterns of heat flow within the Karoo Basin have to be seen in the context of different tectonic settings and kimberlite occurrence: In the northern and central basin parts an elevated heat flow might be related to the occurrence of young (94 Ma and younger) kimberlites (Hielke et al. 2004), the south-western basin part is located in the northern extension of the syntaxis of the Cape Fold Belt (Johnston 2000), and the eastern and south-eastern basin parts build the southernmost extension of the East African rift system (Chorowicz 2005).

The southern Karoo Basin is seen as a promising future target area for geothermal energy exploration in South Africa. The area is characterized by thrust tectonics (Fig. 6) and highly fractured clastic rocks. Sandstones of the Ripon Formation occur at depths

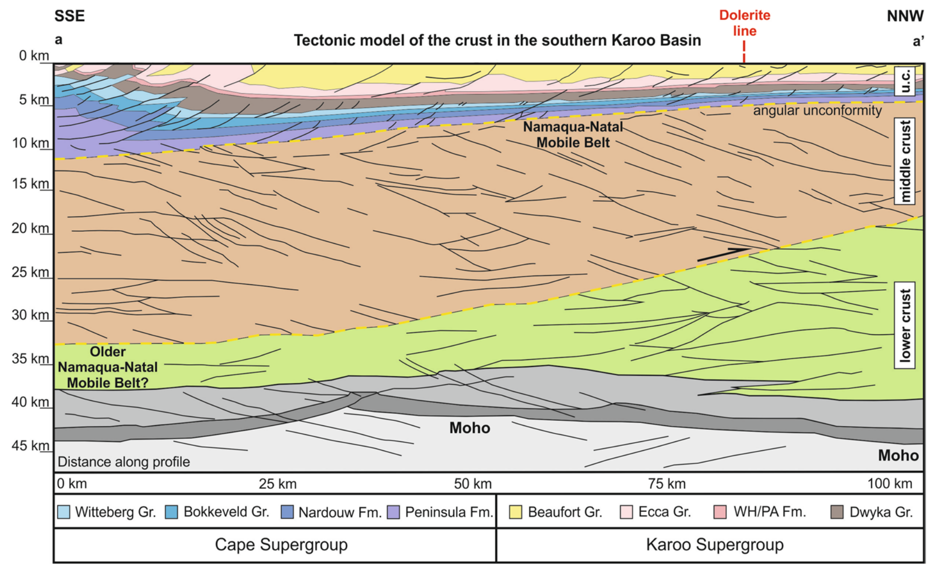


**Fig. 6** SSE–NNW transect through the southern Karoo (for location see Fig. 1) and tectonic model based on interpretation of a seismic reflection profile (modified from Lindeque et al. 2011). The up to 5 km thick Karoo Supergroup is tectonically disrupted by low-angle thrust faults rooted in local décollement horizons in the lower Ecca Group and overlays unconformably the up to 10 km thick wedge of the Cape Supergroup. The underlying mid-crust basement, the Mesoproterozoic Namaqua-Natal Metamorphic Belt (NNMB), reaches a thickness of 13–21 km and the 10–24 km thick lower crust, built by a Paleoproterozoic section of the NNMB or an (?) Archean craton, is bounded by a 2–5 km thick reflective horizon sub-parallel to the Moho. Abbreviations used: *u.c.* upper crust, *Fm.* formation, *Gr.* group, *WH* Whitehill, *PA* Prince Albert

of >3000 m (Fig. 3) and from the borehole KWV-1 data a high thermal conductivity and high specific heat capacity can be assumed. In the region west of East London with deep thermal springs (Steyl et al. 2012), the highly fractured sandstones south of the dolerite line (Fig. 2) might act as transitional systems (Sass and Götz 2012) and can be further enhanced by hydraulic stimulation. In the region northeast of East London, the fractured sandstones are intersected by dolerite sills and here fluid-flow channelling along the intrusion-host rock interfaces might serve as natural enhancement of a petrothermal system that could possibly be operated as an enhanced geothermal system (EGS) by additionally man-made stimulation. However, since information on the deep Karoo aquifer systems is not readily available (Murray et al. 2006), there is a need to address this research gap to provide the necessary information on the hydraulic and hydrochemical properties of reservoir fluids to be integrated in further geothermal exploration strategies.

On a basin-wide scale, the heterogeneity with respect to facies and thickness of prospective sandstone reservoir formations has to be considered for future geothermal exploration activities. However, heat flow in a low permeability basin such as the Karoo is effectively very slow since convective heat transfer is negligible. A predominantly conductive thermal regime can be assumed. As the potential geothermal system would rely on fractures, and these may be very variable in their transmissibility properties across a large area, extrapolating results from a single borehole across the basin remains difficult. Furthermore, until boreholes are drilled to reservoir depth, and fluid has been extracted from a natural or artificial reservoir at an economically sustainable flow rate, no specification can be made about development of or production from the reservoir. However, the initial dataset of the KWV-1 borehole and Ecca Pass section from the southernmost part of the basin identifies this area as the most suitable for ongoing geothermal research.

## Conclusions and outlook

The potential of geothermal energy utilization from the Main Karoo Basin has been assessed by compiling available literature data on the basin's siliciclastic successions, their thickness, lateral extent, depth, as well as using available data on heat flow, geothermal gradient, thermal springs, structural geology and dolerite occurrence and integrating new petro- and thermophysical data, as well as structural and down-hole temperature data obtained from the present study.

Sand- and siltstones of the Permian Ripon Formation were intersected in a deep drill core at a depth between 919.20 and 2294.95 m. Measurements of petro- and thermophysical rock properties of core samples indicate a geothermal resource potential. High thermal conductivities ranging from 3.17 to 3.71 W/(m·K) and a high specific heat capacity are parameters of the geothermal reservoir formation. Although low matrix permeabilities were detected, the reservoir permeability may be enhanced by the joint and fracture system and numerous dolerite sills intersecting the formation with a potential for fluid-flow channelling along the intrusion-host rock interfaces. Temperatures of 80 °C at 2200 m depth indicate a moderately elevated geothermal gradient. Sandstones of the Ripon Formation occurring at >3000 m depths in the southern Eastern Cape region are candidate EGS reservoirs with temperatures >100 °C suitable for electricity production in a binary geothermal power plant.

Thermophysical data gained from an outcrop analogue study of the Ripon Formation exposed about 200 km SW of the studied borehole KWV-1 prove to be of value for a first resource assessment. Similar values of petro- and thermophysical rock properties were collected, classifying the Ripon Formation as a low permeability, fractured reservoir with a high thermal conductivity and a high specific heat capacity. Such petrothermal systems can be exploited and used for electricity production by creating fluid pathways by means of hydraulic stimulation (Breede et al. 2013). Future studies should thus focus on the deep aquifers of the Karoo Basin, e.g. with respect to hydraulic conductivity of the fractures and the influence of dykes and sills intersecting the sandstone formations.

With regard to economic feasibility of electric-power generation in the Karoo, the endeavour to implement geothermal energy as a viable contribution to the future energy mix of South Africa should include feasibility studies on hybrid energy systems such as geothermal-solar-wind systems.

#### Authors' contributions

SAC carried out the logging and petrographical studies of KWV-1. PM carried out the petro- and thermophysical measurements. AEG initiated and leads the KARIN research program. All authors read and approved the final manuscript.

#### Author details

[1] School of Physical and Geographical Sciences, Keele University, Staffordshire ST5 5BG, UK. [2] Institute of Applied Geosciences, Geothermal Science and Technology, Technische Universität Darmstadt, 64287 Darmstadt, Germany.

#### Acknowledgements

This work was funded by the DST-NRF Centre of Excellence for Integrated Mineral and Energy Resource Analysis CIMERA and the Karoo Research Initiative KARIN. The constructive comments of two anonymous reviewers and editor Olaf Kolditz are gratefully acknowledged.

**Competing interests**
The authors declare that they have no competing interests.

Received: 14 March 2016 Accepted: 25 July 2016
Published online: 04 August 2016

**References**

Abdulagatova Z, Abdulagatov IM, Emirov VN. Effect of temperature and pressure on the thermal conductivity of sandstone. Int J Rock Mech Min Sci. 2009;46:1055–71.
Branch T, Ritter O, Weckmann U, Sachsenhofer RF, Schilling F. The Whitehill Formation—a high conductivity marker horizon in the Karoo Basin. S Afr J Geol. 2007;110:465–76.
Breede K, Dzebisashvili K, Liu X, Falcone G. A systematic review of enhanced (or engineered) geothermal systems: past, present and future. Geotherm Energy. 2013;1:4.
Brunt RL, Hodgson DM, Flint SS, Pringle JK, Di Celma C, Prélat A, Grecula M. Confined to unconfined: anatomy of a base of slope succession, Karoo Basin, South Africa. Mar Petrol Geol. 2013;41:206–21.
Calvet E, Prat H. Recent progress in microcalorimetry. Oxford: Pergamon Press; 1963.
Campbell SA. The Ecca type section (Permian, South Africa): an outcrop analogue study of conventional and unconventional hydrocarbon reservoirs. MSc Thesis, Grahamstown: Rhodes University; 2014.
Campbell SA, Lenhardt N, Dippenaar MA, Götz AE. Geothermal energy from the Main Karoo Basin (South Africa): an outcrop analogue study of Permian sandstone reservoir formations. In: EGU Geophysical research abstracts, vol 18. 2016a. p. 115.
Campbell SA, Montenari M, Götz AE. New insights on the Karoo shale gas potential from borehole KZF-1 (Western Cape, South Africa). In: EGU Geophysical research abstracts, vol 18. 2016b. p. 1255.
Catuneanu O. Retroarc foreland systems—evolution through time. J Afr Earth Sci. 2004;38:225–42.
Catuneanu O, Hancox PJ, Rubidge BS. Reciprocal flexural behaviour and contrasting stratigraphies: a new basin development model for the Karoo retroarc foreland system, South Africa. Basin Res. 1998;10:417–39.
Catuneanu O, Hancox PJ, Cairncross B, Rubige BS. Foredeep submarine fans and forebulge deltas: orogenic off-loading in the underfilled Karoo Basin. J Afr Earth Sci. 2002;35:489–502.
Catuneanu O, Wopfner H, Eriksson PG, Cairncross B, Rubidge BS, Smith RMH, Hancox PJ. The Karoo basins of south-central Africa. J Afr Earth Sci. 2005;43:211–53.
Chambefort I, Bignall G. Taupo volcanic zone geothermal systems, New Zealand: exploration, science and development. Geothermics. 2016;59:147–356.
Chevallier L, Musekiwa C, Dhansay T. Geothermal energy potential in South Africa (Geological and socio-economical investigation). In: Progress report of the annual technical programme 2014. Council for Geoscience (CGS) open report 2014-0128.
Chorowicz J. The East African rift system. J Afr Earth Sc. 2005;43:379–410.
Clauser C, Huenges E. Thermal conductivity of rocks and minerals. In: Ahrens TJ, editor. Rock physics and phase relations: a handbook of physical constants. Washington: American Geophysical Union; 1995. p. 105–26.
Cole DI. Evolution and development of the Karoo Basin. In: De Wit MJ, Ransome IGD, editors. Inversion tectonics of the Cape Fold Belt, Karoo and cretaceous basins of Southern Africa. Rotterdam: Balkema; 1992. p. 87–99.
Cornell DH, Thomas RJ, Moen HFG, Reid DL, Moore JM, Gibson RL. The Namaqua-Natal Province. In: Johnson MR, Anhaeusser CR, Thomas RJ, editors. The geology of South Africa. Pretoria, Johannesburg: Geological Society South African Publication, Council for Geoscience; 2006. p. 325–79.
Cox KG. Karoo igneous activity, and the early stages of the break-up of Gondwanaland. In: Story BC, Alabaster T, Pankhurst RJ, editors. Magmatism and the causes of continental break-up, vol. 68. London: Geological Society Special Publication; 1992. p. 137–48.
Craddock JP, McKiernan AW, de Wit MJ. Calcite twin analysis in syntectonic calcite, Cape Fold Belt, South Africa: implications for fold and cleavage formation within a shallow thrust front. J Struct Geol. 2007;29:1100–13.
Decker JE. Preliminary shale gas resource scenarios for the Karoo Basin. Internal PASA report 2011;FG-J04:1–7.
De Wit MJ, Ransome IGD. Regional inversion tectonics along the southern margin of Gondwana. In: de Wit MJ, Ransome IGD, editors. Inversion tectonics of the Cape Fold Belt, Karoo and cretaceous basins of Southern Africa. Rotterdam: Balkema; 1992. p. 15–21.
Duncan RA, Hooper PR, Rehacek J, Marsh JS, Duncan AR. The timing and duration of the Karoo igneous event, southern Gondwana. J Geophys Res. 1997;102:18127–38.
Eggeling L, Kölbel T, Schlagermann P, Münch W. Geothermische Stromerzeugung in Deutschland (Geothermal electricity generation in Germany). Chem Ing Tech. 2011;83:1834–44.
Filomena CM, Hornung J, Stollhofen H. Assessing accuracy of gas-driven permeability measurements: a comparative study of diverse Hassler-cell and probe permeameter devices. Solid Earth. 2014;5:1–11.
Flint SS, Hodgson DM, Sprague AR, Brunt RL, Van der Merwe WC, Figueiredo J, Prélat A, Box D, Di Celma C, Kavanagh JP. Depositional architecture and sequence stratigraphy of the Karoo basin floor to shelf edge succession, Laingsburg depocentre, South Africa. Mar Petrol Geol. 2011;28:658–74.
Folk RL. The distinction between grain size and mineral composition in sedimentary-rock nomenclature. J Geol. 1954;62(4):344–59.
Fuchs S, Schütz F, Förster HJ, Förster A. Evaluation of common mixing models for calculating bulk thermal conductivity of sedimentary rocks: correction charts and new conversion equations. Geothermics. 2013;47:40–52.
Hälbich IW. A tectogenesis of the Cape Fold Belt (CFB). In: Sohnge APG, Hälbich IW, editors. Geodynamics of the Cape Fold Belt, vol 12. Spec Pub Geol Soc S Afr. 1983. p. 165–175.

Hälbich IW. The Cape Fold Belt Orogeny: State of the art 1970s–1980s. In: de Wit MJ, Ransome IGD, editors. Inversion tectonics of the Cape Fold Belt, Karoo and cretaceous basins of Southern Africa, Balkema, Rotterdam. 1992. p. 141–158.
Hancox PJ, Götz AE. South Africa's coalfields—a 2014 perspective. Int J Coal Geol. 2014;132:170–254.
Hielke AJ, de Wit MJ, Thiart C, Dirks PHGM, Viola G, Basson IJ, Anckar E. Preferential distribution along transcontinental corridors of kimberlites and related rocks of Southern Africa. S Afr J Geol. 2004;107:301–24.
Homuth S, Götz AE, Sass I. Lithofacies relation and depth dependency of thermo-physical rock parameters of the Upper Jurassic geothermal carbonate reservoirs of the Molasse Basin. Z Dt Ges Geowiss. 2014;165(3):469–86.
Horváth F, Musitz B, Balázs A, Végh A, Uhrin A, Nádor A, Koroknai B, Pap N, Tóth T, Wórum G. Evolution of the Pannonian basin and its geothermal resources. Geothermics. 2015;53:328–52.
Huenges E. Geothermal energy systems—exploration, development, and utilization. Weinheim: Wiley-VCH; 2010.
James DE, Niu F, Rokosky J. Crustal structure of the Kaapvaal craton and its significance for early crustal evolution. Lithos. 2003;71:413–29.
Johnson MR, Caston DL. The geology of the Kei Mouth area. Explanation to 1:250,000 geology Sheet 3228 Kei Mouth. Pretoria: Council for Geoscience; 1979.
Johnson MR, Van Vauuren CJ, Hegenberger WF, Key R, Shoko U. Stratigraphy of the Karoo supergroup in southern Africa: an overview. J Afr Earth Sci. 1996;23:3–15.
Johnson MR, Van Vuuren CJ, Visser JNJ, Cole DI, de Wickens HV, Christie ADM, Roberts DL. The Foreland Karoo Basin, South Africa. In: Selly RC, editor. African basins. Sedimentary basins of the World 3. Amsterdam: Elsevier Science B.V.; 1997. p. 269–317.
Johnson MR, Van Vuuren CJ, Visser JNJ, Cole DI, de Wickens HV, Christie ADM, Roberts DL, Brandl G. Sedimentary rocks of the Karoo supergroup. In: Johnson MR, Anhaeusser CR, Thomas RJ, editors. The geology of South Africa. Pretoria, Johannesburg: Geol Soc S Afr, Council for Geoscience; 2006. p. 461–99.
Johnston ST. The Cape Fold Belt and syntaxis and the rotated Falkland Islands: dextral transpressional tectonics along the southwest margin of Gondwana. J Afr Earth Sci. 2000;31:51–63.
Jones MQW. Heat flow and heat production in the Namaqua mobile belt, South Africa. J Geophys Res. 1987;92(B7):6273–89.
Jones MQW. Heat flow anomaly in Lesotho: implications for the southern boundary of the Kaapvaal Craton. Geophys Res Lett. 1992;19(20):2031–4.
Jones MQW. Heat flow in South Africa. Pretoria: Handbook of the geological survey no. 14. 1993.
Jones MQW. Heat Flow in Southern Africa and thermal structure of the Kaapvaal lithosphere: Slave-Kaapvaal Workshop. Merrickville; 2001. p. 1–6.
Jourdan F, Féraud G, Bertrand H, Kampunzu AB, Tshoso G, Watkeys MK, Le Gall B. Karoo large igneous province: brevity, origin, and relation to mass extinction questioned by new 40Ar/39Ar age data. Geology. 2005;33:745–8.
Jourdan F, Féraud G, Bertrand H, Watkeys MK, Renne PR. Distinct brief major events in the Karoo large igneous province clarified by new 40Ar/39Ar ages on the Lesotho basalts. Lithos. 2007;98:195–209.
Leith MJ, Trümpelmann F. Well completion report for Southern Oil Exploration Corporation (Pty) Limited of WE 1/66. SOEKOR Report 1967; SV 66.
Lenhardt N, Götz AE. Geothermal reservoir potential of volcaniclastic settings: the Valley of Mexico, Central Mexico. Renew Energ. 2015;77:423–9.
Limberger J, Calcagno P, Manzella A, Trumpy E, Boxem T, Pluymaekers MPD, Van Wees JD. Assessing the prospective resource base for enhanced geothermal systems in Europe. Geoth Energ Sci. 2014;2:55–71.
Lindeque A, De Wit MJ, Ryberg T, Weber M, Chevallier L. Deep crustal profile across the southern Karoo basin and Beattie magnetic anomaly, South Africa: an integrated interpretation with tectonic implications. S Afr J Geol. 2011;114:265–92.
Lund JW, Boyd TL. Direct utilization of geothermal energy 2015 worldwide review. In: Proceedings World Geothermal Congress 2015, Melbourne, Australia, 19–25 April 2015. Melbourne: World Geothermal Congress; 2015.
Marsh JS, Eales HV. The chemistry and petrogenesis of igneous rocks of the Karoo central area, Southern Africa. Spec Publ Geol Soc S Afr. 1984;13:27–67.
McCourt S, Armstrong RA, Grantham GH, Thomas RJ. Geology and evolution of the Natal Belt, South Africa. J Afr Earth Sci. 2006;46:71–92.
McKay MP, Weislogel AL, Fildani A, Brunt RL, Hodgson DM, Flint SS. U-PB zircon tuff geochronology from the Karoo basin, South Africa: implications of zircon recycling on stratigraphic age controls. Int Geol Rev. 2015;57:393–410.
Mountain ED. The geology of the area around East London, Cape Province. An explanation of sheet map 3227D (East London), 3228 (Kei Mouth). Pretoria: Council for Geoscience; 1974.
Muffler P, Cataldi R. Methods for regional assessment of geothermal resources. Geothermics. 1978;7:53–89.
Murray R, Cobbing J, Woodford A, Ravenscroft L, Chevallier L. Groundwater research needs in the Eastern Karoo basin of South Africa. Pretoria: Water Research Commission; 2006. WRC Report No. TT286/06.
Neumann ER, Svensen H, Galerne CY, Planke S. Multistage evolution of dolerites in the Karoo large igneous province, Central South Africa. J Petrol. 2011;52:959–84.
Nguuri TK, Gore J, James DE, Webb SJ, Wright C, Zengeni TG, Gwavana O, Snoke JA, Kaapvaal Seismic Group. Crustal structure beneath southern Africa and its implications for the formation and evolution of the Kaapvaal and Zimbabwe cratons. Geophys Res Lett. 2001;28(13):2501–4.
Popov YA, Pribnow DFC, Sass JH, Williams CF, Burkhardt H. Characterization of rock thermal conductivity by high-resolution optical scanning. Geothermics. 1999;28:253–76.
Rühaak W, Guadagnini A, Geiger S, Bär K, Gu Y, Aretz A, Homuth S, Sass I. Upscaling thermal conductivities of sedimentary formations for geothermal exploration. Geothermics. 2015;58:49–61.
Sass I, Götz AE. Characterization of geothermal reservoirs: a thermofacies concept. Terra Nova. 2012;24:142–7.
Scheiber-Enslin SE, Ebbing J, Webb SJ. New depth maps of the Main Karoo Basin, used to explore the Cape isostatic anomaly, South Africa. S Afr J Geol. 2015;118:225–48.

Schellschmidt R. Vergleichsmessungen der spezifischen Wärmekapazität an Proben aus dem Schweizer Molassebecken mit einem Dynamischen Wärmestrom-Differenz-Kalorimeter. Hannover: Institut für Geowissenschaftliche Gemeinschaftsaufgaben (GGA); 1999. Archiv-Nr. 119564.
Selley RC. Sedimentary basins of the World: the African basins. Amsterdam: Elsevier; 1997.
Senger K, Buckley SJ, Chevallier L, Fagereng Å, Galland O, Kurz TH, Ogata K, Planke S, Tveranger J. Fracturing of doleritic intrusions and associated contact zones: implications for fluid flow in volcanic basins. J Afr Earth Sci. 2015;102:70–85.
Shone RW, Booth PWK. The Cape basin, South Africa: a review. J Afr Earth Sci. 2005;43:196–210.
Smith RMH. A review of stratigraphy and sedimentary environments of the Karoo basin of South Africa. J Afr Earth Sci. 1990;10:117–37.
Smith RMH, Eriksson PG, Botha WJ. A review of the stratigraphy and sedimentary environments of the Karoo-aged basins of Southern Africa. J Afr Earth Sci. 1993;16:143–69.
Somerton WH. Thermal properties and temperature-related behavior of rock-fluid systems. Dev Pet Sci. 1992;37(8):1–257.
Steyl G, van Tonder GJ, Chevallier L. State of the art: fracking for shale gas exploration in South-Africa and the impact on water resources. Pretoria: Water Research Commission; 2012. WRC Report No. KV 294/11.
Svensen H, Corfu F, Polteau S, Hammer Ø, Planke S. Rapid magma emplacement in the Karoo large igneous Province. Earth Planet Sci Lett. 2012;325–326:1–9.
Tankard AJ, Jackson MPA, Eriksson KA, Hobday DK, Hunter, Minter WEL. Crustal evolution of southern Africa: 3.8 billion years of earth history. New York: Springer; 1982.
Tankard A, Welsink H, Aukes P, Newton R, Stettler E. Tectonic evolution of the Cape and Karoo basins of South Africa. Mar Petrol Geol. 2009;26:1379–412.
Tester JW, Drake EM, Golay MW, Driscoll MJ, Peters WA. Sustainable energy—choosing among options. Cambridge: MIT Press; 2005.
Thomas RJ, Cornell DH, Moore JM, Jacobs J. Crustal evolution of the Namaqua-Natal metamorphic province, South Africa. S Afr J Geol. 1993;97(1):8–14.
Tikhomirov VM. The thermal conductivity of rocks and its relationship to density, moisture content, and temperature. Neftianoe Khoziaistvo. 1968;46:36–40 **(in Russian)**.
Trouw RA, de Wit MJ. Relation between the Gondwanide Orogen and contemporaneous intracratonic deformation. J Afr Earth Sci. 1999;28(1):203–13.
Turner BR. Tectonostratigraphical development of the Upper Karoo foreland basin: orogenic unloading versus thermally induced Gondwana rifting. J Afr Earth Sci. 1999;28:215–38.
Veevers JJ. Gondwanaland from 650–500 Ma assembly through 320 Ma merger in Pangea to 185–100 Ma breakup: supercontinental tectonics via stratigraphy and radiometric dating. Earth Sci Rev. 2004;68:1–132.
Veevers JJ, Cole DI, Cowan EJ. Southern Africa: Karoo basin and Cape Fold Belt. In: Veevers JJ, Powell C McA, editors. Permian-Triassic Pangean basins and fold belts along the Panthalassan margin of Gondwanaland, vol 184. GSA Mem; 1994. p. 223–279.
Vosteen HD, Schellschmidt R. Influence of temperature on thermal conductivity, thermal capacity and thermal diffusivity for different types of rock. Phys Chem Earth. 2003;28(9–11):499–509.
Zafar SD, Cutright BL. Texas' geothermal resource base: a raster-integration method for estimating in-place geothermal-energy resources using ArcGIS. Geothermics. 2014;50:148–54.
Zhu J, Hu K, Lu X, Huang X, Liu K, Wu X. A review of geothermal energy resources, development, and applications in China: current status and prospects. Energy. 2015;93:466–83.